

PNNL-33295

Probing f-orbital covalency through the fold angles of transuranium dithiolene complexes

September 2022

Gabriel B Hall
Micah P Prange
Trent R Graham
Herman Cho
Niri Govind
Gregg J Lumetta

DISCLAIMER

This report was prepared as an account of work sponsored by an agency of the United States Government. Neither the United States Government nor any agency thereof, nor Battelle Memorial Institute, nor any of their employees, **makes any warranty, express or implied, or assumes any legal liability or responsibility for the accuracy, completeness, or usefulness of any information, apparatus, product, or process disclosed, or represents that its use would not infringe privately owned rights.** Reference herein to any specific commercial product, process, or service by trade name, trademark, manufacturer, or otherwise does not necessarily constitute or imply its endorsement, recommendation, or favoring by the United States Government or any agency thereof, or Battelle Memorial Institute. The views and opinions of authors expressed herein do not necessarily state or reflect those of the United States Government or any agency thereof.

PACIFIC NORTHWEST NATIONAL LABORATORY
operated by
BATTELLE
for the
UNITED STATES DEPARTMENT OF ENERGY
under Contract DE-AC05-76RL01830

Printed in the United States of America

Available to DOE and DOE contractors from
the Office of Scientific and Technical
Information,
P.O. Box 62, Oak Ridge, TN 37831-0062
www.osti.gov
ph: (865) 576-8401
fox: (865) 576-5728
email: reports@osti.gov

Available to the public from the National Technical Information Service
5301 Shawnee Rd., Alexandria, VA 22312
ph: (800) 553-NTIS (6847)
or (703) 605-6000
email: info@ntis.gov
Online ordering: <http://www.ntis.gov>

Probing f-orbital covalency through the fold angles of transuranium dithiolene complexes

September 2022

Gabriel B Hall
Micah P Prange
Trent R Graham
Herman Cho
Niri Govind
Gregg J Lumetta

Prepared for
the U.S. Department of Energy
under Contract DE-AC05-76RL01830

Pacific Northwest National Laboratory
Richland, Washington 99354

Abstract

The ability of the actinide elements to covalently bond to ligands is not well understood. A computational effort for compounds of the formula $[\text{Cp}_2\text{AnS}_2\text{C}_2\text{H}_2]^{-1,0,+1}$ where An = U, Np, or Pu has shown that the angle between the plane formed by the two sulfurs and the plane formed by the two sulfur atoms and the two carbons converges to $70 - 75^\circ$ when the ligand is in the dithiolate state (-2 charge on the ligand). Upon oxidation of $[\text{Cp}_2\text{NpS}_2\text{C}_2\text{H}_2]^0$ or $[\text{Cp}_2\text{PuS}_2\text{C}_2\text{H}_2]^0$ the electron is removed from the dithiolate rather than the actinide and the dihedral angle is reduced to planarity.

The reaction of $\text{NpCl}_4\text{DME}_2$ with deprotonated benzene dithiol shows an intense color change suggestive of a charge transfer complex. The binding of the benzene dithiol as the dithiolate to the neptunium metal center is supported by visible, infrared and NMR spectroscopies.

Acknowledgments

This research was supported by the Open Call investment under the Laboratory Directed Research and Development (LDRD) Program at Pacific Northwest National Laboratory (PNNL). The computational resources were provided by PNNL Research Computing. PNNL is a multi-program national laboratory operated for the U.S. Department of Energy (DOE) by Battelle Memorial Institute under Contract No. DE-AC05-76RL01830.

Acronyms and Abbreviations

BDT Benzene dithiol

DME Dimethoxy ethane

FEP fluoroethylene polymer

FTIR Fourier transform infrared

NMR Nuclear magnetic Resonance

RBF round bottom flask

TMS tetramethyl silane

Contents

Abstract.....	ii
Acknowledgments.....	iii
Acronyms and Abbreviations.....	iv
Introduction.....	1
Methodology.....	2
Computational Approach.....	2
Synthetic Approach.....	2
Synthesis of $\text{NpCl}_4\text{DME}_2$	2
Synthesis of $\text{Cp}^*_2\text{NpCl}_2$	3
Attempted Synthesis of $\text{Cp}^*_2\text{NpBDT}$	3
Synthesis of homoleptic neptunium complexes.....	3
FTIR Spectroscopy.....	4
NMR spectroscopy.....	4
^1H NMR spectroscopy.....	4
^{13}C NMR spectroscopy.....	4
Results and Discussion.....	5
Computational.....	5
Homoleptic neptunium compounds.....	7
References.....	12

Figures

Figure 1. Computationally investigated structure of $[\text{Cp}_2\text{An}(\text{S}_2\text{C}_2\text{R}_2)]^x$ with the examined fold angle highlighted. Computational structures utilized a molecular charge of -1, 0, or +1 with An = U, Np, or Pu.....	5
Figure 2. Relative energy as a function of fold angle (top) where the energy has been set to 0 for a given oxidation state of the complex. Excess <i>f</i> -orbital occupation (middle), and C-C distance as a function of fold angle (bottom).	6
Figure 3. FTIR spectrum of the solid reaction product of homoleptic neptunium catechol.	7
Figure 4. FTIR spectrum of the solid reaction product of homoleptic neptunium dithiolene.	8
Figure 5. Visible absorption spectrum of the neptunium dithiolate complex.....	9
Figure 6. Chemical structure of benzene dithiolate with magnetically equivalent protons and carbons shown within the same ellipsoid.....	10
Figure 7. ^1H NMR spectra following the reaction of deprotonated benzene dithiol with $\text{NpCl}_4\text{DME}_2$ over time. The data is shown in black, the fits of the individual resonances are shown in green, and the summation of the fits is shown in orange. The chemical shift of two ^1H resonances of benzene 1,2 dithiolate	

bound to Np are 7.9 and 7.1 ppm. The chemical shift of the two ^1H resonances of benzene 1,2 dithiol are 8.1 and 7.7 ppm. The chemical shifts of the ^1H resonances of triethylammonium in solutions of Np are 3.2, 1.8 and 1.5 ppm. The chemical shifts of the ^1H resonances of triethylamine are at 3.2 and 1.7 ppm.10

Figure 8. ^{13}C NMR spectra following the aromatic carbons of BDT upon reaction with $\text{NpCl}_4\text{DME}_2$. The data is shown in black, the fits of the individual resonances are shown in green, and the summation of the fits is shown in orange. The asterisks mark a trace impurity found in the reaction mixture. The chemical shift of three ^{13}C resonances of benzene 1,2 dithiolate bound to Np are 144.1, 129.7, and 122.3 ppm. The chemical shift of the two ^{13}C resonances of benzene 1,2 dithiol are 131.3 and 126.9 ppm. The chemical shifts of the ^{13}C resonances of triethylammonium in solutions of Np are 46.4 and 10.1 ppm. The chemical shifts of the ^{13}C resonances of triethylamine are at 47 and 12.4 ppm.11

Tables

Table 1. Energy optimized fold angle, spin multiplicity and assigned metal oxidation state for $\text{Cp}_2\text{AnS}_2\text{C}_2\text{H}_2$ complexes.6

Introduction

The role that *f*-electrons play in the chemical bonding of the actinide elements is not well understood.(Pace et al. 2021) Historically, the actinide elements were thought to bond in a similar manner to their lanthanide analogues. For the lanthanides, the 4*f* orbitals are contracted with a shorter radius than the fully occupied 5*d* orbitals. Consequently, the 4*f* orbitals are blocked from spatial overlap with ligands, and do not exhibit significant metal-ligand covalency. Since the 5*d* orbitals are occupied in the lanthanides, they do not participate in covalent bonding, resulting in primarily ionic interactions. However, for the actinide elements multiple phenomena occur that allow for increased covalent bonding. The 5*f* orbitals radially extend far enough to not be entirely blocked from overlap by the 6*d* orbitals, and the energy difference between the 6*d* and 5*f* orbitals is lessened leading to partial occupancy of both orbital sets.(Pace et al. 2021) This leads to a scenario where not only can the actinide elements exhibit covalent bonding with the 5*f* orbitals, but the 6*d* orbitals as well. Consequently, the lanthanides are poor non-radioactive surrogates for studying *f*-orbital covalency in the actinide series. Combined with a dearth of known actinide compounds containing non-innocent ligand architectures it is difficult to ascertain what factors drive covalent bonding in the actinides. The hazard associated with handling transuranic elements has caused the primary focus of actinide research to be highly application based with few fundamental studies relative to the transition metal series. Thus, the extensive studies which have been performed for the transition metal series with non-innocent ligands from the 1960s through present day are simply not abundant for the actinide series.

Dithiolenes as a ligand class first came to prominence in the early 1960s when they revolutionized the understanding of covalent bonding in the transition metal series.(Eisenberg and Gray 2011) The ability of dithiolene ligands to act “non-innocently” challenged the then held theories on metal ligand interaction and shaped our modern understanding of ligand field theory. The general ligand architecture of $[\text{Cp}_2\text{M}(\text{S}_2\text{C}_2\text{R}_2)]^X$, has been used extensively to study the redox interplay of transition metals with the dithiolene ligands.(Enemark et al. 2004; Cooney et al. 2004; Cranswick et al. 2007; Joshi et al. 2003; Stein et al. 2018; Fourmigué 1998) In particular, the dihedral angle between the plane formed by the metal and the two sulfur atoms against the plane formed by the two sulfur atoms and the two attached carbon atoms has been used to infer information about the oxidation state of the dithiolate ligand and the degree to which it is stabilizing the metal oxidation state as an oxidized dithiolene ligand.

Classically, the transplutonium actinide elements are thought to demonstrate very little covalent bonding, however recent work suggests that covalency may play a role in the bonding of transplutonium complexes.(Goodwin et al. 2019; Silver et al. 2017; White, Dan, and Albrecht-Schmitt 2019) Dithiolene *f*-element compounds are relatively unstudied with only a few examples of U dithiolene compounds coming from Germany in the late 1960s and early 1970s,(Dietzsch and Karl-marx-universitat 1967; Zimmer and Lieser 1971b; 1971a) and a limited number of examples since 2000.(Thérèse Arliguie et al. 2004; Roger, Belkhiri, et al. 2005; Therese Arliguie, Fourmigué, and Ephritikhine 2000; Belkhiri et al. 2006) All are U or lanthanide analogues. The “fold-angle” has been shown to vary with U oxidation state; furthermore, considerably more metal-sulfur covalent interaction is observed for U^{III} over Ln^{III}.(Roger, Belkhiri, et al. 2005; Meskaldji et al. 2010) Thus, this ligand architecture may offer a mechanism to study electronic communication in the actinide series with covalently bound ligands. This ligand class offers potential advantages to studying covalency in transuranic elements:

- The “fold-angle” response to metal-ligand electronic communication offers an easily measured geometric change with respect metal-ligand covalency

- Modification of dithiolene substituents allows tuning ligand electron donation, and consequently covalency

To explore the possibility of using these ligands, we have undertaken an experimental effort supported by a computational study to determine the application of the dithiolene ligands to studying covalency in transuranic chemistry.

Methodology

Computational Approach

For computational studies, Cp ligands are utilized in place of the methylated Cp* ligands to conserve computational time and simplify relaxations. Further the dithiolene ligand was truncated to its simplest form, S₂C₂H₂. All DFT computations were performed in the NWChem computational package, (Aprà et al. 2020; Valiev et al. 2010) utilizing the PBE0 exchange-correlation functional. (Adamo and Barone 1999) The Stuttgart/Cologne group of basis sets were utilized with energy consistent pseudopotentials replacing 60 core electrons for the actinide elements. (Dolg et al. 1993; Küchle et al. 1994; Cao, Dolg, and Stoll 2003) For the light elements (H, C, S) the 6-311G** basis set was used. (Clark et al., n.d.; Gordon et al. 1982; Spitznagel et al., n.d.; Hariharan and Pople 1973; Francl et al. 1982; Hehre, Ditchfield, and Pople 1972; Ditchfield, Hehre, and Pople 1971) CASSCF calculations were performed with OpenMolcas. (Fdez. Galván et al. 2019)

To optimize geometries a z-matrix was utilized which allowed all parameters to be optimized except the C-S-S-An dihedral angle which was fixed. A linear transit was performed in which the dihedral angle was fixed at a given angle from 0° to 90° in a stepwise fashion while all other parameters were allowed full relaxation.

Synthetic Approach

Organic solvents, triethyl amine, trimethyl silyl chloride, benzene dithiol, the potassium pentamethylcyclopentadienide in THF solution and catechol were obtained from Sigma Aldrich. Organic solvents, and triethyl amine were ordered as anhydrous solvents. Organic solvents were further purified by drying over molecular sieves for at least 24 hours followed by removal of residual air by freeze-pump-thawing. Glassware was heated in a vacuum oven under reduced pressure until utilized for a given synthesis. Unless otherwise noted, all synthetic steps were performed with a dual manifold Schlenk line under an Ar atmosphere. Argon gas was purified by passing it through 5A molecular sieves and a copper catalyst to remove residual moisture and oxygen respectively.

Synthesis of NpCl₄DME₂

To produce pure Np^{IV} source material for synthesis of NpCl₄DME₂, a literature procedure was followed in which the valence was adjusted in 2 M HCl with hydroxyl amine followed by fluoride precipitation, removal of fluoride with boric acid, and purification by anion exchange. (Cary et al. 2018) From here, the synthesis of NpCl₄DME₂ roughly followed literature procedure developed elsewhere. (Reilly et al. 2014; Whitefoot et al. 2021) Briefly, in a typical synthesis 200 mg of NpCl₄ would be dried to a residue under Ar gas and resuspended in DME followed by addition

of trimethyl silyl chloride. The reaction was heated to 45-50 °C with stirring. After a period of 4 hours, the solution was cannula filtered to a fresh flask with additional DME added to wash the solid precipitate generated from the reaction of trimethyl silyl chloride with residual moisture. The resulting solution was evaporated to dryness under vacuum and rinsed with cold dimethyl ether to obtain a nearly quantitative yield. Resuspension of the solid in DME yielded a visible spectrum consistent with what has previously been reported in the literature.

Synthesis of $\text{Cp}^*_2\text{NpCl}_2$

The synthesis of $\text{Cp}^*_2\text{NpCl}_2$ was conducted in benzene under air free conditions. The starting material, $\text{NpCl}_4\text{DME}_2$ was reacted with 2.1 molar equivalents of pentamethylcyclopentadienide in THF at 50 °C for five days. The resulting darkly colored solution was filtered by cannula filtration to a fresh vial and the volume reduced to a viscous oil. The oil was resuspended in benzene and stored at -20 °C overnight which afforded a precipitate and a lightly colored purple solution. The liquid was decanted and the solid rinsed with dried diethyl ether for a 19 % yield.

Attempted Synthesis of $\text{Cp}^*_2\text{NpBDT}$

Isolated solids of $\text{Cp}^*_2\text{NpCl}_2$ were dissolved in THF in an inerted round bottom flask. In a separate round bottom flask, two equivalents of benzene dithiol dissolved in THF and two equivalents of triethylamine relative to the benzene dithiol were added. A slightly yellow colored precipitate was observed to form. The solution of $\text{Cp}^*_2\text{NpCl}_2$ was then added to the flask containing BDT in a dropwise fashion at 0 °C. The flask was allowed to stir overnight at room temperature with the color of the solution darkening over time. The solution was filtered and stored at -20 °C for 24 hours which produced small darkly colored crystals. Upon exposure to atmosphere to mount a crystal for single crystal x-ray diffraction analysis the sample rapidly decomposed. Due to the reactive nature of the solid and the time-consuming synthesis, further attempts to remake this compound for alternative characterization were abandoned.

Synthesis of homoleptic neptunium complexes

Two separate routes synthetic routes were pursued. In the first route, BDT was dissolved in DME and deprotonated with triethyl amine. This caused the precipitation of a slightly yellow colored solid. $\text{NpCl}_4\text{DME}_2$ was dissolved separately in DME and added to the reaction flask containing the deprotonated BDT solid. The BDT salt was precipitated as a salt, but upon introduction of the $\text{NpCl}_4\text{DME}_2$ solution, the color changed to a deep purple color with a visible change in the solid occurring which we are attributing to the dissolution of the BDT and precipitation of Et_3NHCl . No noticeable change was noted between reaction times of 4 hours and 24 hours.

In the second methodology, BDT dissolved in DME was added to a solution of $\text{NpCl}_4\text{DME}_2$ and allowed to stir for 10 minutes. No precipitation was observed and only a faint color change occurred. Upon the dropwise addition of triethyl amine a deep purple color change occurred accompanied by precipitation of a light colored solid.

Under both synthetic pathways it was found that the resulting product was stable for a period of at least a week when stored under an inerted atmosphere as either a solid or in solution. Upon exposure to air, the synthesized compound would change in color from purple to a tan color and precipitate if in solution. The structure of this complex is not confirmed but is tentatively assigned as $[\text{NpBDT}_3][\text{Et}_3\text{NH}]_2$. An analogous procedure was used to produce the homoleptic neptunium catechol compound.

FTIR Spectroscopy

FTIR spectra were collected inside of a radiological fumehood on a Bruker ALPHA II spectrometer equipped with a single bounce diamond ATR plate. Presented spectra are the average of at least 24 scans with a resolution of 2 cm^{-1} . Measurements were performed under ambient temperature and atmosphere.

NMR spectroscopy

NMR experiments utilized $[\text{NpBDT}_3]^{2-}$ synthesized by the above procedure. Samples prepared in deuterated pyridine and CDCl_3 , showed decomposition over the time period of the experiment and are not being discussed herein.

For the NMR experiments utilizing DME solvent, the above synthetic procedure was utilized, and the crude reaction mixture was analyzed without purification. The samples were transferred in an air free manner into FEP NMR tube liners procured from Wilmad Glass which were stoppered with a septum and subjected to 4 pump purge cycles utilizing Ar gas. The FEP NMR tube liners were then placed in 8 mm glass nmr tubes which were further purged with Ar gas.

^1H NMR spectroscopy

Single pulse, direct excitation ^1H NMR spectra were collected on a 7.05 T superconducting magnet, corresponding to a ^1H Larmor frequency of 300.130 MHz. The instrument is equipped with a Redstone console from TecMag Inc. ^1H NMR spectra were acquired with an acquisition time of 819.2 ms enumerated with 8192 points, a sweep width of 10000 Hz, a collection of 16 transients, a recycle delay of 60 s, and a 71.8 μs excitation pulse equivalent to approximately a $\pi/2$ pulse length. The pulse length was calibrated using a sample of anhydrous methanol, and the ^1H chemical shift was externally referenced to the chemical shift of tetramethylsilane ($\delta = 0$ ppm) in deuterated chloroform. The ^1H NMR spectra were processed in Mestrenova (version 14.01-23559, released 2019-06-07, Mestrelab Research S.L.), where the free induction decay was zero-filled three times to 65536 points and 5 Hz of exponential line broadening was applied. ^1H NMR spectra were also predicted in Chem Draw Professional (Perkin Elmer, v. 16.0.0.82(68)).

^{13}C NMR spectroscopy

Proton-decoupled ^{13}C NMR spectra were also collected on the 7.05 T NMR spectrometer. At 7.05 T, the Larmor frequency of ^{13}C is 75.468 MHz. The proton-decoupled ^{13}C NMR spectra were acquired with an acquisition time of 409.6 ms enumerated with 16384 points, a recycle delay of 10 minutes, a 7.3 μs pulse equivalent to a $\pi/2$ pulse length. The $\pi/2$ pulse length was calibrated using a sample of anhydrous methanol. The ^{13}C chemical shift was externally referenced to the chemical shift of tetramethylsilane ($\delta = 0$ ppm) in deuterated chloroform. Proton decoupling was performed using the WALTZ90 scheme using 71.8 μs ($\pi/2$) pulses on the proton channel. The proton decoupled ^{13}C NMR spectra were processed in Mestrenova, where 2 Hz of exponential line broadening was applied. ^{13}C NMR spectra were also predicted in Chem Draw Professional.

Results and Discussion

Computational

A computational study was undertaken to determine if the dithiolenes through their fold angle (Figure 1) could be used as reporter ligands to study the covalency between actinide ions and sulfur bearing ligands. It should be noted that the computationally examined structure is likely not the most synthetically accessible compound due to ligand modifications made to simplify the calculations. The methyl groups have been removed from the synthetically attempted pentamethylcyclopentadienide analog, and the dithiolene ligand has been simplified to R = H in order to simplify the computations.

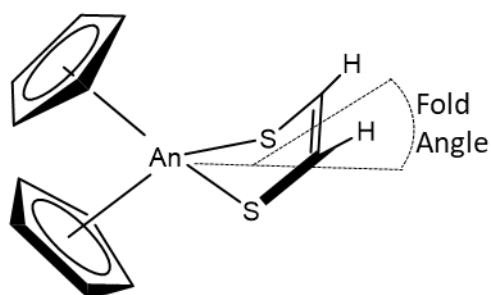


Figure 1. Computationally investigated structure of $[\text{Cp}_2\text{An}(\text{S}_2\text{C}_2\text{R}_2)]^x$ with the examined fold angle highlighted. Computational structures utilized a molecular charge of -1, 0, or +1 with An = U, Np, or Pu.

Computational efforts were limited to the compound $\text{Cp}_2\text{AnS}_2\text{C}_2\text{H}_2$ where the An was U, Np, or Pu. A molecular charge of +1, 0, or -1 was assigned to the complex, which corresponds to an actinide oxidation state of +3, +4, or +5 if the dithiolate ligand remains in the reduced -2 state. For the case of uranium, the fold angle is largely independent of the uranium oxidation state as shown in Table 1. The potential energy well for variation in fold angle is relatively shallow as shown in Figure 2, and the influence of crystal packing in synthesized samples would likely have a larger impact than the electronic interaction between the dithiolene ligand and the uranium center. However, for Np, there is a steep dependence between the fold angle and the Np oxidation state. For $[\text{CpNpS}_2\text{C}_2\text{H}_2]^{-1}$ and $[\text{CpNpS}_2\text{C}_2\text{H}_2]^0$ the fold angle is near identical to the uranium compounds and the formal oxidation states of Np^{III} and Np^{IV} based on excess *f*-orbital occupation are consistent with the results obtained for the uranium series. However, upon oxidation of the complex to $[\text{CpNpS}_2\text{C}_2\text{H}_2]^{+1}$ the fold angle becomes planar and the electron is removed from the dithiolene ligand rather than from the metal center. It appears this is a mechanism by which the dithiolene ligand is stabilizing the overall complex charge and upon oxidation of the dithiolene ligand the fold angle is decreased, breaking covalency between the actinide and the ligand in order to prevent further loss of electron density from the dithiolene ligand.

For the two plutonium oxidation states examined a similar trend to the Np case is seen, where upon oxidation to the state of $[\text{CpPuS}_2\text{C}_2\text{H}_2]^{+1}$ the fold angle is reduced to planarity when the ligand is oxidized in place of the actinide center.

Table 1. Energy optimized fold angle, spin multiplicity and assigned metal oxidation state for $\text{Cp}_2\text{AnS}_2\text{C}_2\text{H}_2$ complexes.

	Net molecular charge	Optimized fold angle (degrees)	Spin multiplicity	Assigned actinide oxidation state
U	+1	75	2	U^{V}
	0	72	3	U^{IV}
	-1	70	4	U^{III}
Np	+1	0	5	Np^{IV}
	0	72	4	Np^{IV}
	-1	74	5	Np^{III}
Pu	+1	0	6	Pu^{IV}
	0	70	5	Pu^{IV}

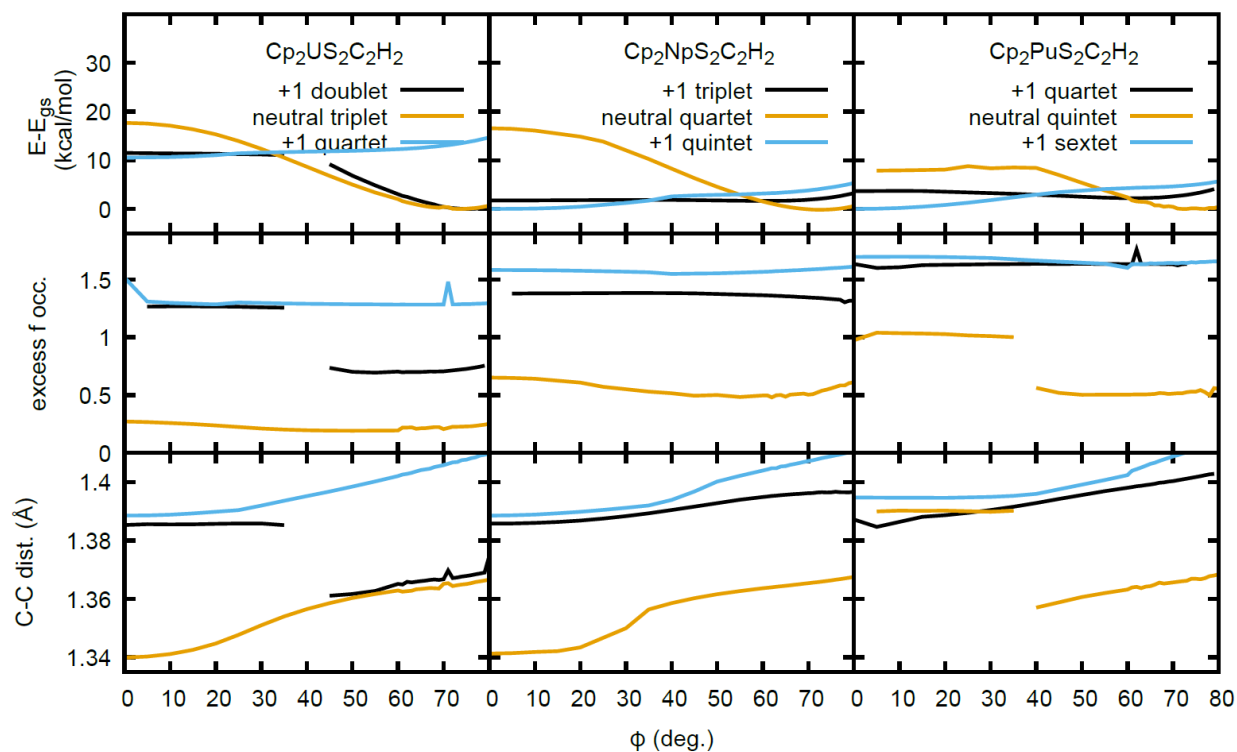


Figure 2. Relative energy as a function of fold angle (top) where the energy has been set to 0 for a given oxidation state of the complex. Excess f -orbital occupation (middle), and C-C distance as a function of fold angle (bottom).

Homoleptic neptunium compounds

The infrared spectrum of the homoleptic neptunium catechol compound, Figure 3, shows a small residual amount of unreacted catechol at 1618, and 1596 cm^{-1} . The main feature of interest is the resonance at 1574 cm^{-1} which is attributable to the C=C stretching frequency. This is a decreased stretching frequency by comparison to what we observed for deprotonated catechol (1600 cm^{-1}) but is slightly higher in frequency than what has been reported in the literature for homoleptic $(\text{Et}_3\text{NH})_2\text{V}(\text{cat})_2\text{CH}_3\text{CN}$ of 1569 cm^{-1} . (Cooper, Bai Koh, and Raymond 1982) This is consistent with the catechol being bound directly to the neptunium center through the oxygen atoms.

When the same reaction was performed but with benzene dithiol in place of catechol, the resulting infrared spectrum, Figure 4, shows a C=C resonance at 1560 cm^{-1} with a shoulder at 1560 cm^{-1} . This again is consistent with the C=C resonance shifting due to binding to the metal center due to the shift from a value of 1571 cm^{-1} for unbound benzenedithiol.

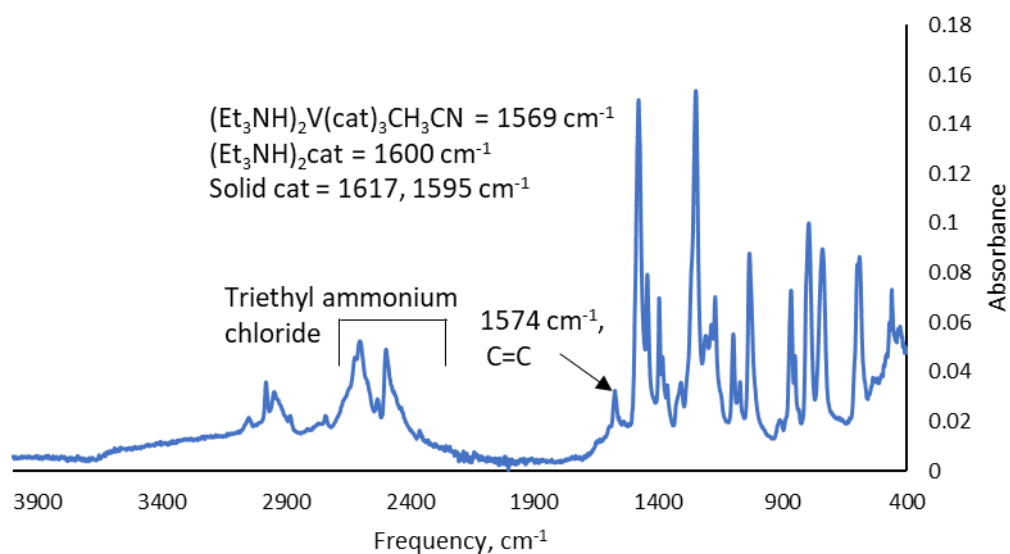


Figure 3. FTIR spectrum of the solid reaction product of homoleptic neptunium catechol.

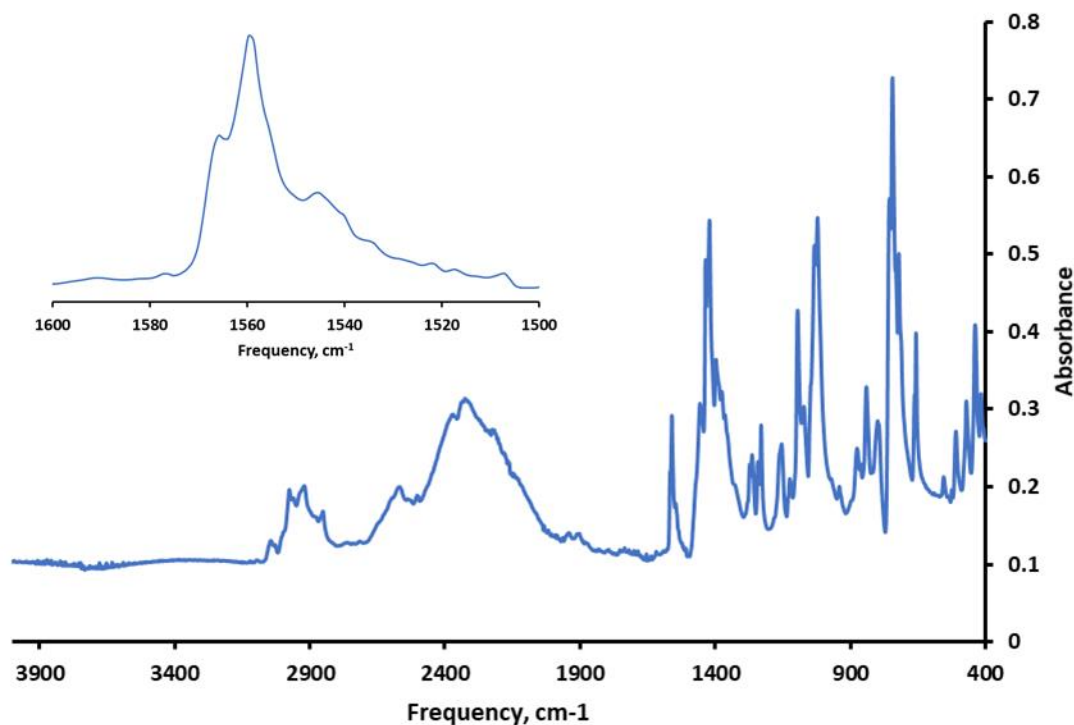


Figure 4. FTIR spectrum of the solid reaction product of homoleptic neptunium dithiolene.

The most convincing evidence for electronic communication between the dithiolene ligand and the neptunium center is the intense color change that is observed upon mixing and the resulting visible absorbance spectrum (Figure 5). Benzene dithiol is a faint yellow color, including after deprotonation with triethyl amine. The $\text{NpCl}_4\text{DME}_2$ starting material is a light orange in color and the visible absorbance spectrum has sharp absorbances characteristic of the $f \rightarrow f$ transitions of the actinide elements. Upon reaction between the deprotonated benzene dithiolene and $\text{NpCl}_4\text{DME}_2$ the solution immediately turns a very dark purplish red color. The visible absorption spectrum shows a single broad absorbance at short wavelength which is more characteristic of the d-block or a charge transfer occurring.

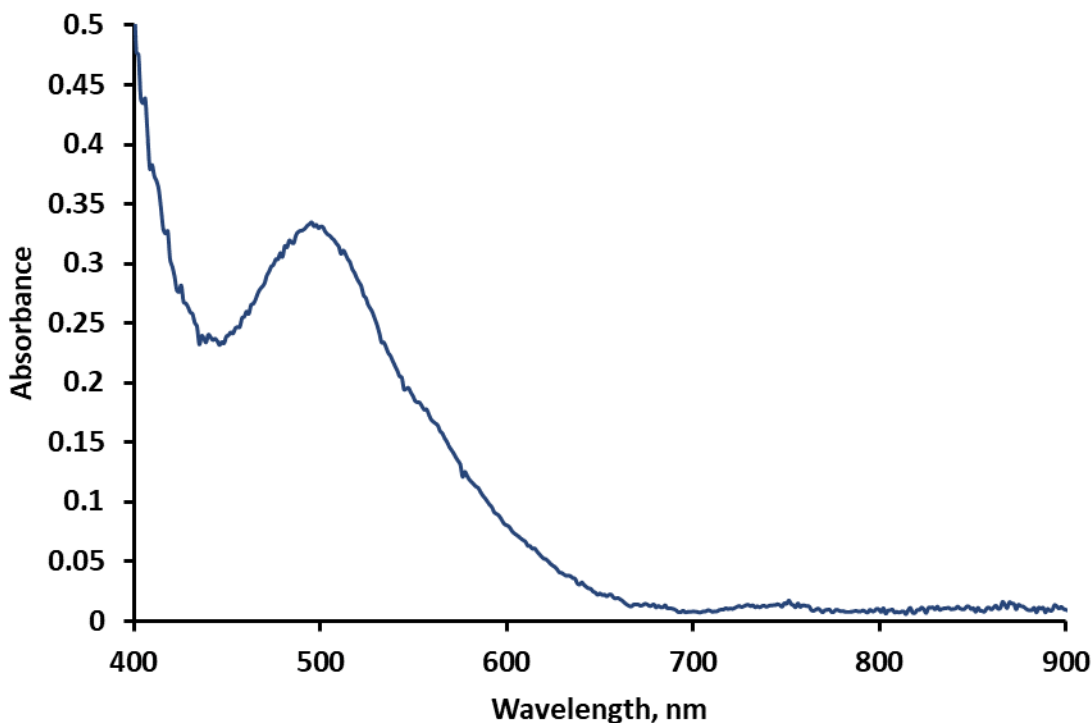


Figure 5. Visible absorption spectrum of the neptunium dithiolate complex.

The ^1H and ^{13}C NMR spectra were initially collected for DME solutions containing either benzene dithiol or triethylamine in the absence of Np. These spectra are then compared to ^1H and ^{13}C NMR spectra obtained with the reaction product of $\text{NpCl}_4\text{DME}_2$. In the reaction mixture, benzene dithiol is deprotonated to form benzene dithiolate and triethylamine is protonated to become triethylammonium. The chemical structure of benzene dithiolate and the anticipated number of distinct proton and carbon resonances are shown in Figure 6. Based on the molecular structure of benzene dithiolate, two proton resonances and three carbon resonances are anticipated.

The ^1H spectrum of benzene 1,2 dithiol in DME (Figure 7) shows two resonances for the aromatic protons before reaction with neptunium. After reaction with neptunium in DME bearing triethylamine, the resonances are slightly broadened and the two resonances are shifted to lower chemical shift values. The ^1H resonances of triethylamine are also sensitive to formation of triethylammonium, with the resonance assigned to the CH_2 groups splitting into two resonances, and the emergence of a resonance in the aromatic region which shifts to lower frequencies over time. Based on the variation of the chemical shift of this peak, the labile resonance is assigned to the HNR_3 of triethylammonium.

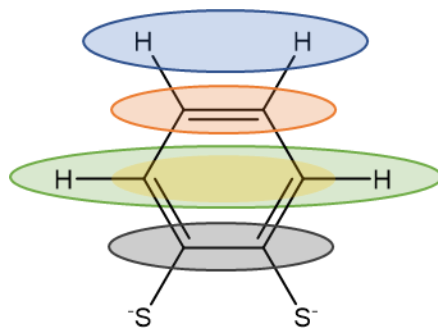


Figure 6. Chemical structure of benzene dithiolate with magnetically equivalent protons and carbons shown within the same ellipsoid.

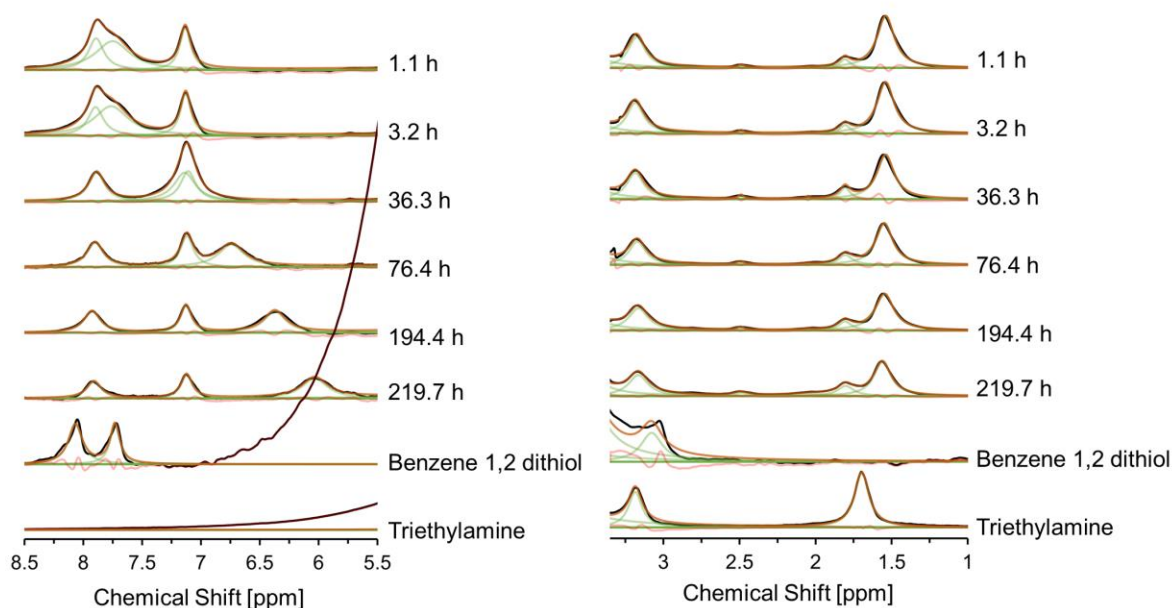


Figure 7. ^1H NMR spectra following the reaction of deprotonated benzene dithiol with $\text{NpCl}_4\text{DME}_2$ over time. The data is shown in black, the fits of the individual resonances are shown in green, and the summation of the fits is shown in orange. The chemical shift of two ^1H resonances of benzene 1,2 dithiolate bound to Np are 7.9 and 7.1 ppm. The chemical shift of the two ^1H resonances of benzene 1,2 dithiol are 8.1 and 7.7 ppm. The chemical shifts of the ^1H resonances of triethylammonium in solutions of Np are 3.2, 1.8 and 1.5 ppm. The chemical shifts of the ^1H resonances of triethylamine are at 3.2 and 1.7 ppm.

The corresponding ^{13}C spectra of the reference solutions and reaction mixture are shown in Figure 8. Comparing between the spectra of the reference solutions of the benzene 1,2 dithiol and triethylamine in the absence of Np with the reaction mixture leads to observations consistent with the ^1H NMR spectra. Note that in the solution with the protonated benzene dithiol, only two resonances are observed corresponding to the aromatic carbons, whereas three are predicted based on Figure 6. This is likely due to the ^{13}C environments shown in orange and yellow in Figure 6 having resonances with near equivalent chemical shielding tensors leading to overlapping peaks. Upon complexation to neptunium two relatively sharp resonances are present upfield which we believe belong to the carbons from the orange and yellow environment. Upon complexation to neptunium, an additional broad resonance occurs at

145 ppm which we hypothesize to be associated with the alpha carbons relative to the dithiolate (gray in Figure 6).

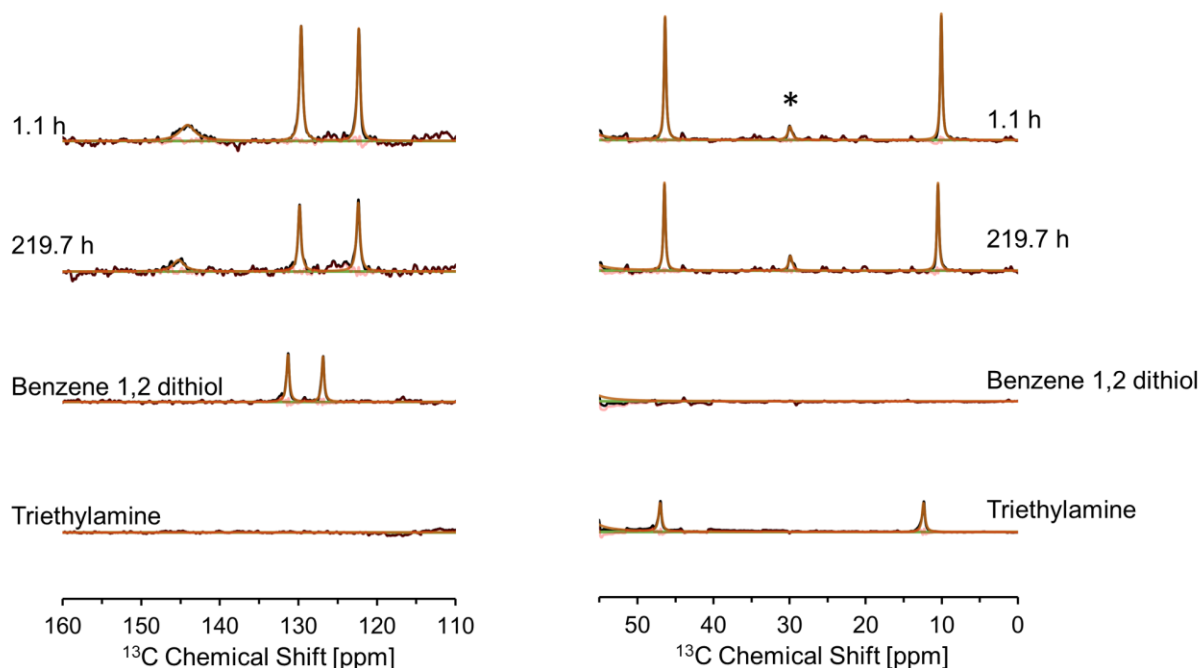


Figure 8. ^{13}C NMR spectra following the aromatic carbons of BDT upon reaction with $\text{NpCl}_4\text{DME}_2$. The data is shown in black, the fits of the individual resonances are shown in green, and the summation of the fits is shown in orange. The asterisks mark a trace impurity found in the reaction mixture. The chemical shift of three ^{13}C resonances of benzene 1,2 dithiolate bound to Np are 144.1, 129.7, and 122.3 ppm. The chemical shift of the two ^{13}C resonances of benzene 1,2 dithiol are 131.3 and 126.9 ppm. The chemical shifts of the ^{13}C resonances of triethylammonium in solutions of Np are 46.4 and 10.1 ppm. The chemical shifts of the ^{13}C resonances of triethylamine are at 47 and 12.4 ppm.

Given that only two proton resonances and three carbon resonances are observed in the ^1H and ^{13}C spectra of the reaction mixture with Np, we hypothesize that the dithiolate ligands bound to the neptunium center either result in equivalent proton and carbon environments when comparing between dithiolate ligands in the Np solvation shell. Alternatively, if the dithiolate ligands in the Np solvation shell are inequivalent, the observation of only two proton environments in the ^1H spectra would necessitate fast interconversion between dithiolate ligand fold angles in the Np solvation shell which result in the observation of ensemble resonances corresponding to the two observed proton environments and three observed carbon environments of benzene 1,2 dithiolate in the presence of Np. The alternative hypothesis of fast interconversion between fold angles is consistent with prior work with homoleptic uranium dithiolate complexes which showed fast interconversion at room temperature due to ring inversion. (Roger, Arliguie, et al. 2005) It should be noted that when an attempt was made to collect the NMR spectrum of benzene dithiol which was deprotonated with triethyl amine in the absence of Np, the dithiolate precipitated in under 10 minutes which prevented collection of the NMR spectrum. Thus, these shifted aromatic resonances of the aromatic ring on the dithiolate are from interaction with the neptunium center, because the solubility (activity) of benzene dithiolate in an unbound state is negligible.

References

- Adamo, Carlo, and Vincenzo Barone. 1999. "Toward Reliable Density Functional Methods without Adjustable Parameters: The PBE0 Model." *Journal of Chemical Physics* 110 (13): 6158–70. <https://doi.org/10.1063/1.478522>.
- Aprà, E., E. J. Bylaska, W. A. de Jong, N. Govind, K. Kowalski, T. P. Straatsma, M. Valiev, et al. 2020. "NWChem: Past, Present, and Future." *Journal of Chemical Physics* 152 (18). <https://doi.org/10.1063/5.0004997>.
- Arliquie, Therese, Marc Fourmigue, and Michel Ephritikhine. 2000. "The First Dithiolene Complexes of an F-Element, Including the Cyclooctatetraene Derivative." *Organometallics* 19 (2): 109–11.
- Arliquie, Thérèse, Pierre Thuéry, Marc Fourmigué, and Michel Ephritikhine. 2004. "Monocyclooctatetraenyl(Dithiolene)Uranium Compounds." *European Journal of Inorganic Chemistry*, no. 22: 4502–9. <https://doi.org/10.1002/ejic.200400403>.
- Belkhiri, Lotfi, Thérèse Arliquie, Pierre Thuéry, Marc Fourmigué, Abdou Boucekkine, and Michel Ephritikhine. 2006. "Investigation of the Dithiolene Ligand Conformation in Analogous U(IV)/U(V) Complexes: X-Ray Diffraction and Density Functional Theory Analysis of the U···(C=C) Interaction." *Organometallics* 25 (11): 2782–95. <https://doi.org/10.1021/om060083d>.
- Cao, Xiaoyan, Michael Dolg, and Hermann Stoll. 2003. "Valence Basis Sets for Relativistic Energy-Consistent Small-Core Actinide Pseudopotentials." *Journal of Chemical Physics* 118 (2): 487–96. <https://doi.org/10.1063/1.1521431>.
- Cary, Samantha K., Maksim Livshits, Justin N. Cross, Maryline G. Ferrier, Veronika Mocko, Benjamin W. Stein, Stosh A. Kozimor, Brian L. Scott, and Jeffrey J. Rack. 2018. "Advancing Understanding of the +4 Metal Extractant Thenoyltrifluoroacetate (TTA); Synthesis and Structure of $M^{IV}TTA_4$ ($M^{IV} = Zr, Hf, Ce, Th, U, Np, Pu$) and $M^{III}(TTA)_4^-$ ($M^{III} > I$)." *Inorganic Chemistry* 57 (7): 3782–97. <https://doi.org/10.1021/acs.inorgchem.7b03089>.
- Clark, Timothy, Jayaraman Chandrasekhar, Gunther W Spitznagel, Paul Von, and Ragu6 Schleyer. n.d. "Efficient Diffuse Function-Augmented Basis Sets for Anion Calculations. III.* The 3-21+G Basis Set for First-Row Elements, Li-F."
- Cooney, J. Jon A., Matthew A. Cranswick, Nadine E. Gruhn, Hemant K. Joshi, and John H. Enemark. 2004. "Electronic Structure of Bent Titanocene Complexes with Chelated Dithiolate Ligands." *Inorganic Chemistry* 43 (25): 8110–18. <https://doi.org/10.1021/ic049207+>.
- Cooper, Stephen R, Yun Bai Koh, and Kenneth N. Raymond. 1982. "Synthetic, Structural, and Physical Studies of Bis(Triethylammonium) Tris(Catecholato)Vanadate(IV), Potassium Bis(Catecholato)Oxovanadate(IV), and Potassium Tris(Catecholato)Vanadate(III)." *Journal of the American Chemical Society* 104: 5092–5102.
- Cranswick, Matthew A., Alice Dawson, J. Jon A. Cooney, Nadine E. Gruhn, Dennis L. Lichtenberger, and John H. Enemark. 2007. "Photoelectron Spectroscopy and Electronic Structure Calculations of d^1 Vanadocene Compounds with Chelated Dithiolate Ligands: Implications for Pyranopterin Mo/W Enzymes." *Inorganic Chemistry* 46 (25): 10639–46. <https://doi.org/10.1021/ic701338s>.
- Dietzsch, Wolfgang, and Sektion Chemie Der Karl-marx-universitat. 1967. "Dithiolenchelate Des Urans Mit Cis-1,2-Dicyanoathylen-1,2-Dithiolat." *Inorg. Nucl. Chem. Letters* 5: 635–38.
- Ditchfield, R., W. J. Hehre, and J. A. Pople. 1971. "Self-Consistent Molecular-Orbital Methods. IX. An Extended Gaussian-Type Basis for Molecular-Orbital Studies of Organic Molecules." *The Journal of Chemical Physics* 54 (2): 720–23. <https://doi.org/10.1063/1.1674902>.

- Dolg, Michael, Hermann Stoll, Heinzwerner Preuss, and Russell M Pitzer. 1993. "Relativistic and Correlation Effects for Element 105 (Hahnium, Ha): A Comparative Study of M and MO (M = Nb, Ta, Ha) Using Energy-Adjusted Ab Initio Pseudopotentials." *The Journal of Physical Chemistry* 97 (22): 5852–59. <https://doi.org/10.1021/j100124a012>.
- Eisenberg, Richard, and Harry B Gray. 2011. "Noninnocence in Metal Complexes : A Dithiolene Dawn." *Inorganic Chemistry*, 9741–51.
- Enemark, John H., J. Jon A. Cooney, Jun Jieh Wang, and R. H. Holm. 2004. "Synthetic Analogues and Reaction Systems Relevant to the Molybdenum and Tungsten Oxotransferases." *Chemical Reviews* 104 (2): 1175–1200. <https://doi.org/10.1021/cr020609d>.
- Fdez. Galván, Ignacio, Morgane Vacher, Ali Alavi, Celestino Angeli, Francesco Aquilante, Jochen Autschbach, Jie J. Bao, et al. 2019. "OpenMolcas: From Source Code to Insight." *Journal of Chemical Theory and Computation*. American Chemical Society. <https://doi.org/10.1021/acs.jctc.9b00532>.
- Fourmigué, Marc. 1998. "Mixed Cyclopentadienyl/Dithiolene Complexes." *Coordination Chemistry Reviews* 178–180: 823–64. [https://doi.org/10.1016/s0010-8545\(98\)00104-0](https://doi.org/10.1016/s0010-8545(98)00104-0).
- Francl, Michelle M., William J. Pietro, Warren J. Hehre, J. Stephen Binkley, Mark S. Gordon, Douglas J. DeFrees, and John A. Pople. 1982. "Self-Consistent Molecular Orbital Methods. XXIII. A Polarization-Type Basis Set for Second-Row Elements." *The Journal of Chemical Physics* 77 (7): 3654–65. <https://doi.org/10.1063/1.444267>.
- Goodwin, Conrad A.P., Jing Su, Thomas E. Albrecht-Schmitt, Anastasia V. Blake, Enrique R. Batista, Scott R. Daly, Stefanie Dehnen, et al. 2019. "[Am(C5Me4H)3]: An Organometallic Americium Complex." *Angewandte Chemie - International Edition* 58 (34): 11695–99. <https://doi.org/10.1002/anie.201905225>.
- Gordon, Mark S, J Stephen Binkley, Ib A John Pople, Ib J William Pietro, Warren J Hehre, J S Binkley, J A Pople, and W J Hehre. 1982. "Self-Consistent Molecular-Orbital Methods. 22. Small Split-Valence Basis Sets for Second-Row Elements." *Am. Chem. Soc. Vol. 104*. UTC. <https://pubs.acs.org/sharingguidelines>.
- Hariharan, P C, and J A Pople. 1973. "The Influence of Polarization Functions on Molecular Orbital Hydrogenation Energies." *Theoret. Chim. Acta (Berl.)*. Vol. 28. Springer-Verlag.
- Hehre, W. J., K. Ditchfield, and J. A. Pople. 1972. "Self-Consistent Molecular Orbital Methods. XII. Further Extensions of Gaussian-Type Basis Sets for Use in Molecular Orbital Studies of Organic Molecules." *The Journal of Chemical Physics* 56 (5): 2257–61. <https://doi.org/10.1063/1.1677527>.
- Joshi, Hemant K., J. Jon A. Cooney, Frank E. Inscore, Nadine E. Gruhn, Dennis L. Lichtenberger, and John H. Enemark. 2003. "Investigation of Metal-Dithiolate Fold Angle Effects: Implications for Molybdenum and Tungsten Enzymes." *Proceedings of the National Academy of Sciences of the United States of America* 100 (7): 3719–24. <https://doi.org/10.1073/pnas.0636832100>.
- Küchle, W., M. Dolg, H. Stoll, and H. Preuss. 1994. "Energy-Adjusted Pseudopotentials for the Actinides. Parameter Sets and Test Calculations for Thorium and Thorium Monoxide." *The Journal of Chemical Physics* 100 (10): 7535–42. <https://doi.org/10.1063/1.466847>.
- Meskaldji, Samir, Lotfi Belkhir, Thérèse Arliguie, Marc Fourmigué, Michel Ephritikhine, and Abdou Boucekkine. 2010. "Density Functional Theory Investigations of the Homoleptic Tris(Dithiolene) Complexes [M(Dddt)3]-q (Q=3, 2; M = Nd³⁺ and U^{3+/4+}) Related to Lanthanide(LII)/Actinide(LII) Differentiation." *Inorganic Chemistry* 49 (7): 3192–3200. <https://doi.org/10.1021/ic902135t>.
- Pace, Kristen A., Vladislav v. Klepov, Anna A. Berseneva, and Hans Conrad zur Loye. 2021. "Covalency in Actinide Compounds." *Chemistry - A European Journal* 27 (19): 5835–41. <https://doi.org/10.1002/chem.202004632>.

- Reilly, Sean D., Jessie L. Brown, Brian L. Scott, and Andrew J. Gaunt. 2014. "Synthesis and Characterization of $\text{NpCl}_4(\text{DME})_2$ and $\text{PuCl}_4(\text{DME})_2$ Neutral Transuranic An(IV) Starting Materials." *Journal of the Chemical Society. Dalton Transactions* 43 (4): 1498–1501. <https://doi.org/10.1039/c3dt53058b>.
- Roger, Mathieu, Thérèse Arliguie, Pierre Thuéry, Marc Fourmigué, and Michel Ephritikhine. 2005. "Homoleptic Tris(Dithiolene) and Tetrakis(Dithiolene) Complexes of Uranium(IV)." *Inorganic Chemistry* 44 (3): 594–600. <https://doi.org/10.1021/ic049054q>.
- Roger, Mathieu, Lotfi Belkhiri, Pierre Thuéry, Thérèse Arliguie, Marc Fourmigué, Abdou Boucekkine, and Michel Ephritikhine. 2005. "Lanthanide(III)/Actinide(III) Differentiation in Mixed Cyclopentadienyl/ Dithiolene Compounds from X-Ray Diffraction and Density Functional Theory Analysis." *Organometallics* 24 (21): 4940–52. <https://doi.org/10.1021/om050329z>.
- Silver, Mark A., Samantha K. Cary, Alejandro J. Garza, Ryan E. Baumbach, Alexandra A. Arico, Gregory A. Galmin, Kuan Wen Chen, et al. 2017. "Electronic Structure and Properties of Berkelium Iodates." *Journal of the American Chemical Society* 139 (38): 13361–75. <https://doi.org/10.1021/jacs.7b05569>.
- Spitznagel, Gunther W, Timothy Clark, Paul Von, Rag& Schleyer, and Warren J Hehre. n.d. "An Evaluation of the Performance of Diffuse Function-Augmented Basis Sets for Second Row Elements, Na-C1*."
- Stein, Benjamin W., Jing Yang, Regina Mtei, Nicholas J. Wiebelhaus, Dominic K. Kersi, Jesse Lepluart, Dennis L. Lichtenberger, John H. Enemark, and Martin L. Kirk. 2018. "Vibrational Control of Covalency Effects Related to the Active Sites of Molybdenum Enzymes." *Journal of the American Chemical Society* 140 (44): 14777–88. <https://doi.org/10.1021/jacs.8b08254>.
- Valiev, M., E. J. Bylaska, N. Govind, K. Kowalski, T. P. Straatsma, H. J.J. van Dam, D. Wang, et al. 2010. "NWChem: A Comprehensive and Scalable Open-Source Solution for Large Scale Molecular Simulations." *Computer Physics Communications* 181 (9): 1477–89. <https://doi.org/10.1016/j.cpc.2010.04.018>.
- White, Frankie D., David Dan, and Thomas E. Albrecht-Schmitt. 2019. "Contemporary Chemistry of Berkelium and Californium." *Chemistry - A European Journal* 25 (44): 10251–61. <https://doi.org/10.1002/chem.201900586>.
- Whitefoot, Megan A., Diana Perales, Matthias Zeller, and Suzanne C. Bart. 2021. "Synthesis of Non-Aqueous Neptunium(III) Halide Solvates from NpO_2 ." *Chemistry - A European Journal* 27 (72): 18054–57. <https://doi.org/10.1002/chem.202103265>.
- Zimmer, L., and K.H. Lieser. 1971a. "Isomere Uranyl-Chelate Mit Dithiolat-Liganden." *Inorg. Nucl. Chem. Letters* 7: 563–67.
- . 1971b. "Uranyl-Bis(Dithiolat)-Komplexe Mit Pyridin-n-Oxid, Triphenylphosphinoxid Und Triphenylarsinoxid Als Ligand." *Inorg. Nucl. Chem. Letters* 7: 1163–68.

Pacific Northwest National Laboratory

902 Battelle Boulevard
P.O. Box 999
Richland, WA 99354

1-888-375-PNNL (7665)

www.pnnl.gov